ARTICLE

Journal of Materials Chemistry
www.rsc.org/materials

Electrostatic self-assembly of structured gold nanoparticle/polyhedral oligomeric silsesquioxane (POSS) nanocomposites

Joseph B. Carroll, Benjamin L. Frankamp, Sudhanshu Srivastava and Vincent M. Rotello*

Department of Chemistry, The University of Massachusetts, Amherst, MA 01003, USA.
E-mail: rotello@chem.umass.edu

Received 18th September 2003, Accepted 27th November 2003
First published as an Advance Article on the web 5th January 2004

Hybrid inorganic/organic composite materials composed of gold nanoparticles of varying size (1.5 and 6.8 nm) and polyhedral oligomeric silsesquioxane (POSS) units were created using electrostatic self-assembly. Carboxylic acid-functionalized mixed monolayer protected gold clusters (MMPCs) were mixed with trimethyl quaternary ammonium-functionalized POSS units, providing well-ordered aggregates. The aggregates were characterized with transmission electron microscopy (TEM) and small angle X-ray scattering (SAXS), revealing an increase in average interparticle spacing upon assembly with POSS. This increase in spacing was shown to influence the surface plasmon resonance band of the larger 6.8 nm Au nanoparticles as characterized by UV/Vis spectroscopy.

Introduction

The ability to engineer materials at the nanoscale level is crucial in the development of new technologies.[1] Directed self-assembly of nanometer-sized building blocks using non-covalent interactions (*e.g.* hydrogen bonding, acid/base proton transfer, and electrostatic forces) has been proven as an effective way to create tailored materials.[2] Nanoparticles are among the most common and versatile building blocks employed in the creation of these materials. Among the many attributes of nanoparticle scaffolds is their ability to be synthetically manipulated in terms of size and surface functionality, often exhibiting intrinsic functionality such as magnetism, photoluminescence, or catalytic activity. This utility can be extended through non-covalent assembly methods that possess the ability to regulate spacing and structure in the resulting nanocomposite systems.

Polyhedral oligomeric silsesquioxanes (POSS®)[3] such as octa-ammonium POSS® (**OA-POSS**, Fig. 1) are cubic-shaped molecules that contain an inorganic siloxane core (6 Å^3) surrounded by eight functional, organic groups.[4] The POSS core units are stable to a variety of conditions, making them useful modifiers in a variety of applications including non-ablatives, atomic oxygen resistance, and fire protection.[5] The nature of the organic groups dictates the solution and solid-state chemical properties of these POSS units. These side chains have been manipulated in order to incorporate POSS moieties into both polymeric and ceramic systems.[6] Covalently attaching POSS units to polymer backbones has been shown to be effective in enhancing both the thermal and mechanical properties of polymer-based materials.[7] Recently, POSS molecules have been employed as non-covalent modifiers in various materials and surfaces, for example, polymers,[8] surface modification,[9] and the preparation of thin films.[10]

Our lab recently reported an assembly strategy that combined three-point hydrogen bonding between POSS units and gold nanoparticles. We identified a two-stage assembly strategy in which POSS units functionalized with hydrogen bonding recognition units were used to assemble Au nanoparticles into discrete aggregates.[11] In this research, diamidopyridine-functionalized POSS units undergo an initial hydrogen bonding interaction with a complementary thymine-functionalized Au nanoparticle followed by subsequent aggregation and crystallization of the POSS moieties producing well-defined, spherical, hybrid aggregates of varying size, featuring uniform interparticle spacings. Extending this methodology to POSS units with recognition functionality on every corner of the cage

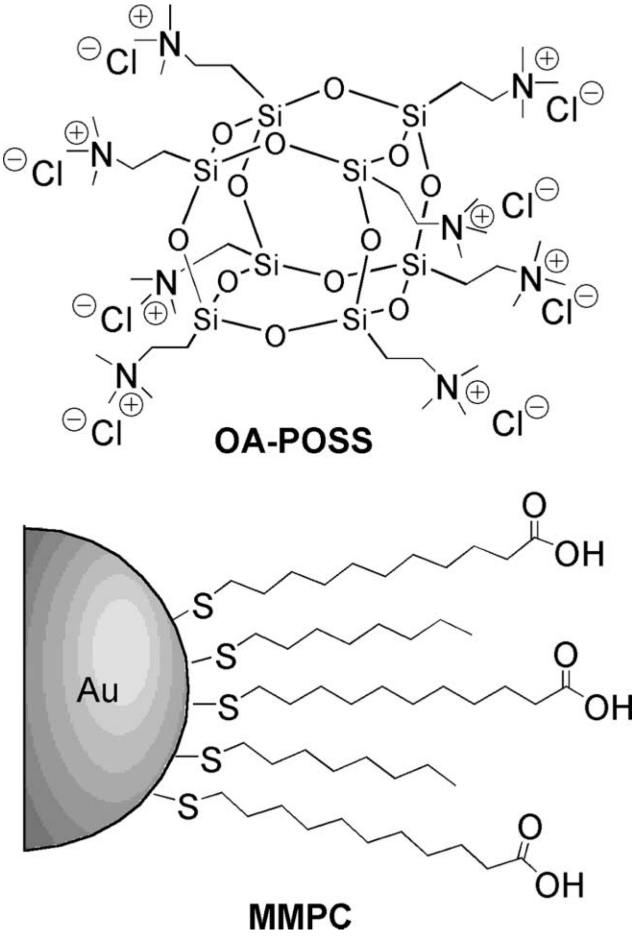

Fig. 1 Octa-ammonium POSS (**OA-POSS**) with carboxylic acid-functionalized **MMPC**.

DOI: 10.1039/b311423f

provides an alternative assembly motif that should provide different aggregate morphologies.

Recently, Chujo and co-workers have demonstrated that polydisperse, palladium(II) acetate nanoparticles self-assemble with quartenary ammonium-functionalized POSS units resulting in large, spherical aggregates (70 nm, mean diameter).[12] Extension of this concept to the production of extended networks of monodisperse nanoparticles with defined interparticle spacing opens the door to the preparation of ordered bulk materials with interesting optical,[13] electronic,[14] and magnetic properties.[15] Using similar methods we have been able to manipulate silica–metal scaffolds creating novel hybrid materials capable of olefin reduction catalysis[16] and the immobilization of proteins.[17]

In this paper, we report the preparation of ordered networks of electrostatically assembled POSS/Au nanoparticles. Carboxylic acid-functionalized nanoparticles (**MMPC**s) of varying size (1.5 and 6.8 nm) were assembled with octa-ammonium POSS units resulting in well-ordered, extended structures. These assemblies feature uniform interparticle spacings consistent with the POSS diameter as characterized by transmission electron microscopy (TEM) and small angle X-ray scattering (SAXS). UV/Vis spectroscopy was used to observe the surface plasmon resonance band of the larger 6.8 nm nanoparticles before, during, and after POSS assembly, demonstrating direct modulation of the optical properties of the aggregates.

Methodology

The quaternary ammonium functionalities on the POSS units act as electrostatic cross-linking agents as is shown in Scheme 1. To effectively cross-link the nanoparticle building blocks, an excess of the POSS was used to ensure complete aggregation. Initially as the nanoparticles are dropped into the POSS solution, a single POSS monolayer is expected to form on the nanoparticles. Over time, the system can reorganize to maximize electrostatic interactions resulting in a single POSS layer between particles (*vide infra*), forming small aggregates and eventually films. In our studies, the 1.5 nm nanoparticles began to assemble and precipitate shortly upon addition into the POSS solution, whereas the larger 6.8 nm particles precipitated over a period of a few days. Obviously, very few (1 or 2) POSS molecules are needed to link two 1.5 nm gold particles together given their relative similarity in size. In contrast, an increased number of POSS units (6–10) are needed to cross-link the 6.8 nm particles; the steric and entropic demands of reorganization process in these larger particles is evidenced by the slower assembly times.

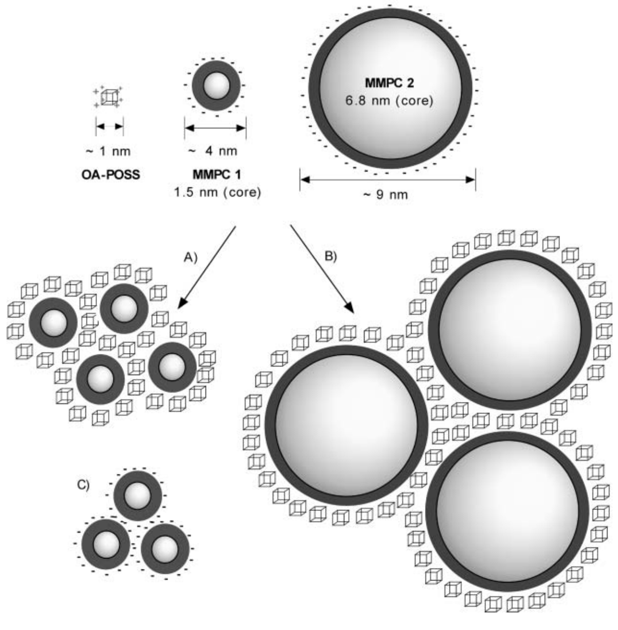

Scheme 1 Schematic illustration showing the electrostatic self-assembly between the (A) 1.5 nm core (*ca.* 4 nm with monolayer) **MMPC 1** and (B) 6.8 nm core (*ca.* 9 nm with monolayer) **MMPC 2** with **OA-POSS** (*ca.* 1 nm). (C) Control **MMPC 1** precipitated from hexanes assembled through acid–acid dimerization.

Preparation and characterization of POSS/Au assemblies

Samples of electrostatically coupled nanocomposites were prepared by dropping solutions of **MMPC**s (1.5 and 6.8 nm) in THF/MeOH (1 mg ml^{-1}) into a solution of octa-ammonium POSS in MeOH/H_2O (10 mg ml^{-1}). The 1.5 nm particles began to assemble within 2 min as the solution became visibly turbid, indicative of an aggregation process (Scheme 1). The 6.8 nm particles assembled more slowly (*vide supra*), precipitating fully after 48 h.

Transmission electron microscopy was used to characterize the nanocomposite morphology during assembly. Micrographs taken of the 1.5 nm (Fig. 2b,c) and 6.8 nm (Fig. 2e,f) gold nanoparticles assembled with **OA-POSS** reveal the presence of extended networks with some evidence of medium range ordering.

Control micrographs of both **MMPC**s, **1** (Fig. 2a) and **2** (Fig. 2d), precipitated from hexanes in the absence of POSS exhibited limited structure, with aggregation presumably arising from carboxylic acid dimerization between the acid functional groups on the nanoparticles during deposition onto the TEM grid.

SAXS studies were performed to quantify the interparticle spacing within the POSS/Au aggregates. Turbid solutions of **OA-POSS/MMPC** assemblies were allowed to precipitate onto Kapton® films. Excess solvent was decanted off and the films were allowed to dry under argon before SAXS analysis. The control sample – the nanoparticle alone – was prepared through precipitation using hexanes leaving a film of nanoparticles spaced only through their respective monolayers. Control 1.5 nm particles exhibited one distinct peak at 0.191 q, revealing an average interparticle spacing of *ca.* 3.2 nm (Fig. 3).[18] This value is consistent with the expected interparticle spacing for 1.5 nm Au nanoparticles separated only by their monolayers. Upon assembly with **OA-POSS**, a decrease in the principle q spacing to 0.145 is observed correlating to an interparticle spacing of 4.3 nm. This 1.1 nm increase in interparticle spacing is consistent with the average diameter observed for one octa-ammonium POSS unit (*ca.* 1 nm). This result suggests that only a single layer of POSS is required in order to assemble the nanoparticles, consistent with the cross-linking assembly represented in Scheme 1. The shoulder observed at 0.275 q can be indicative of some degree of medium range ordering in these hybrid aggregates. A similar shoulder can be observed in the control sample by converting the intensity to a log scale; however, it is dampened significantly due to the more random spacing provided by COOH dimerization. Significant sharpening of this peak in the POSS assembled sample suggests a more ordered system, consistent with TEM evidence. The final peak observed at around 0.400 q corresponds to a spacing of *ca.* 1.57 nm and is most likely due to POSS–POSS scattering interactions rather than the form factor of the gold nanoparticle core as reported earlier.†.

SAXS studies of control **MMPC 2** (alone) reveal the presence of one distinct peak at 0.0857 q which correlates to a 7.32 nm interparticle spacing between nanoparticles (Fig. 4).

---

† SAXS analysis of POSS–POSS scattering interactions available.

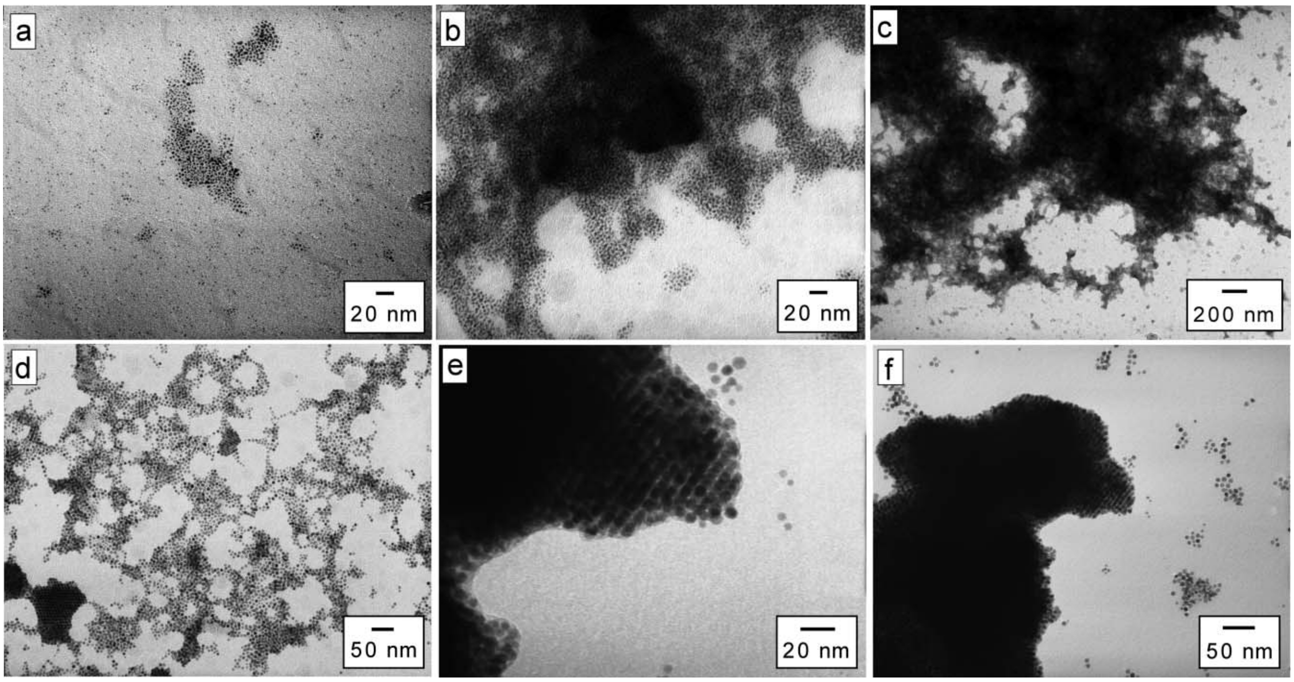

Fig. 2 TEM image of (a) control 1.5 nm **MMPC 1** (alone) precipitated from hexanes shows limited aggregation. TEM images of 1.5 nm **MMPC 1** with **OA-POSS** units reveal the presence of large, extended, hybrid networks at both (b) high and (c) low magnifications. (d) Control images of the larger 6.8 nm **MMPC 2** reveal the presence of weakly-formed Au nanoparticle networks (acid–acid dimerization). TEM images of 6.8 nm **MMPC 2** with **OA-POSS** units reveal the presence of very densely packed POSS/Au structures at both (e) high and (f) low magnifications.

This distance agrees well with the projected interparticle spacing between the 6.8 nm core Au nanoparticles with an acid-functionalized monolayer. Upon assembly with POSS the major peak shifts to a lower *q* value of 0.0738 corresponding to an interparticle distance of 8.51 nm. This 1.2 nm increase in interparticle spacing is similar to the 1.1 nm increase in spacing observed with the 1.5 nm as a result of the electrostatic assembly of one layer of POSS on the periphery of the nanoparticle monolayer.

UV/Visible spectroscopy (UV/Vis) of OA-POSS/MMPC 2 assemblies (solution and solid-state)

Large gold particles (>5 nm) exhibit a surface plasmon resonance (SPR) that is based both on the size of the metal core and the interparticle spacing (dipolar coupling) between the nanoparticles.[19] Using UV/Vis spectroscopy we monitored the SPR of **MMPC 2** before, during, and after assembly to investigate what effect POSS spacing might have on the optical properties of our system. A kinetic experiment was performed measuring the SPR shifts during the aggregation process. Solutions of 6.8 nm particles (0.05 mg ml^{-1} in MeOH) were added dropwise to a solution of **OA-POSS** (5 mg ml^{-1} in MeOH) at ambient temperatures, spectra were aquired over different time intervals (Fig. 5). Overall, a distinctive red-shift in the SPR occurs from 529 to 541 nm accompanied by a decrease in inensity as the assembly precipitates from solution (Fig. 5a).[20]

During the initial 4 h, no change was observed in the SPR band at 529 nm; however, after 24 h, a red-shift (533 nm) and decrease in the intensity of the SPR band occurred. Over time the size of the aggregates in solution becomes increasingly

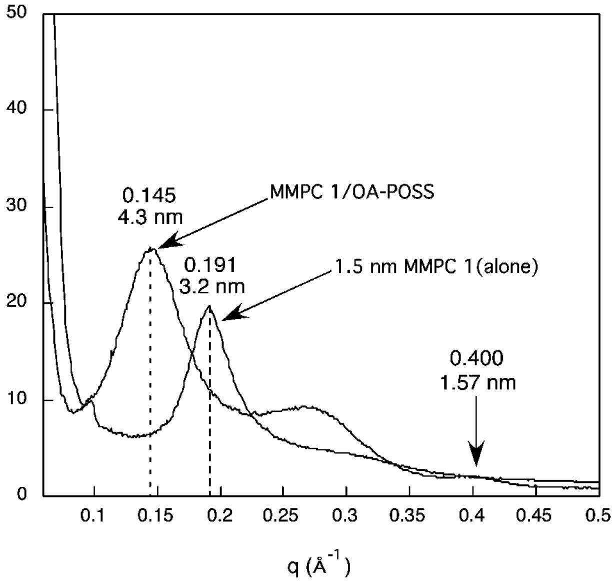

Fig. 3 SAXS plots of **MMPC 1** alone and in aggregates assembled with **OA-POSS** units.

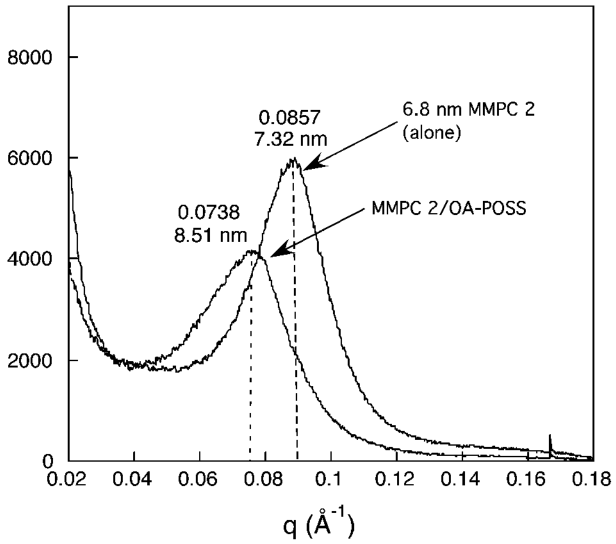

Fig. 4 SAXS plots of **MMPC 2** alone and in aggregates assembled with **OA-POSS** units.

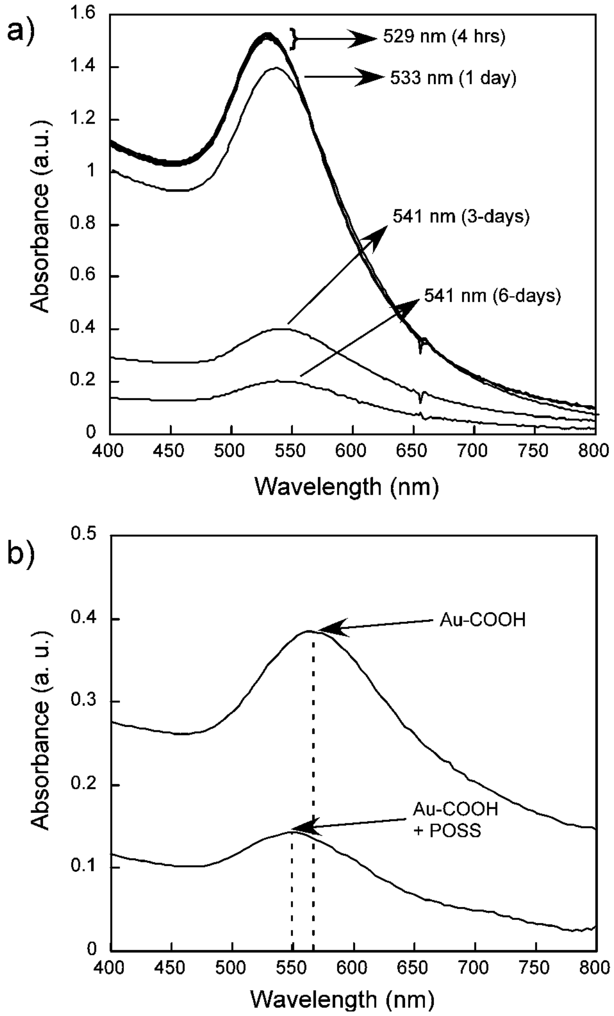

Fig. 5 (a) UV/Vis spectrum of **OA-POSS/MMPC 2** in solution (MeOH) showing a time-dependent red-shift in the SPR band of the Au nanoparticles. (b) UV/Vis spectrum of **OA-POSS/MMPC 2** aggregates and control **MMPC 2** (alone) on Mylar® films showing a blue-shift in the SPR band of the Au nanoparticles.

larger causing a further red-shift in SPR due to an increase in scattering[20] which is in good agreement with Mie theory.[21] As precipitation continued over the next several days, the intensity of the SPR band continued to decrease while shifting to longer wavelengths, finally becoming stable at 541 nm.

The UV/Vis spectrum taken of the aggregates in the solid-state reveals a characteristic blue-shift to lower wavelengths (Fig. 5b). This shift occurs because as two nanoparticles are brought closer together they have a very strong dipole–dipole interaction[22] shifting the SPR band to higher wavelengths. As we increase the interparticle spacing between the nanoparticles using our POSS units, dipole–dipole interaction are weakened resulting in a blue-shift in the SPR band[23] in the UV/Vis spectrum.

In summary, electrostatic self-assembly was used to create hybrid inorganic/organic materials composed of gold nanoparticles (1.5 and 6.8 nm) and polyhedral oligomeric silsesquioxane (POSS) units. Upon assembly, well-ordered, extended aggregates were observed as witnessed by TEM. SAXS was used to quantify the spacing between the Au nanoparticles showing a *ca.* 1 nm increase in spacing upon assembly *versus* a control sample. As a result of this increase in interparticle spacing the SPR of the 6.8 nm particles shifts to higher wavelengths in solution. In the solid-state the SPR shifts to lower wavelengths due to a decrease in particle–particle dipolar interactions in line with Mie theory for these types of systems.

Experimental section

All starting materials were purchased from Aldrich Chemical Company and used without further purification. Hydrogen tetrachloroaurate(III) hydrate was purchased from Strem Chemicals, Inc. Tetrahydrofuran was distilled from sodium and benzophenone under an argon atmosphere. Hexane solvent was distilled before use. Distilled water and methanol solvents were used without any other purification.

Syntheses of 1.5 and 6.8 nm, carboxylic acid-functionalized gold nanoparticles

The octa-ammonium POSS® units were purchased from Hybrid Plastics, Inc. and were used without any further purification.

The 1.5 nm gold nanoparticles used in this research (**MMPC 1**) were prepared through standard Brust–Schiffrin[24] methodology. Subsequent Murray place exchange[25] of mercaptoundecanoic acid into the octanethiol-functionalized gold nanoparticles resulted in *ca.* 50% acid coverage.

The larger 6.8 nm gold nanoparticles (**MMPC 2**) were prepared by a heat treatment method.[23] In summary, the standard Brust reaction mixture is evaporated without removing the tetraoctylammonium bromide (TOAB) and dried completely under reduced pressure. The black solid obtained was heat-treated at 165 °C, at a heating rate of 2 °C min^{-1} and held at this temperature for 30 min. The thermally 'ripened' product was dissolved in toluene and washed with methanol to remove excess ligand and TOAB. The 6.8 nm particles were then place-exchanged with mecaptoundecanoic acid in toluene resulting in precipitation. The precipitate was then washed with successively more polar solvents (dichloromethane, chloroform, ethanol, methanol, water) sectioning the reaction mixture by percent coverage of acid functionality. In our studies, methanol-soluble, acid-functionalized gold nanoparticles were used.

Materials characterization

TEM was carried out using a JEOL 2000FX operating at 200 keV. Volumes of the turbid solutions were then dropcast onto 300 mesh Cu TEM grids for TEM analysis.

SAXS measurements were performed on a Rigaku RU-H3R rotating anode X-ray diffractometer equipped with an Osmic multilayer focusing optic and an evacuated Statton-type scattering camera, with $q = (4\pi/\lambda)\sin(\theta/2)$, where θ is twice the Bragg angle. The incident beam wavelength, λ, was 0.154 nm, corresponding to 8 keV Cu Kα radiation. Scattering patterns were acquired with a 10 × 15 cm^2 Fuji BAS-2500 image plate scanner, and intensity profiles were obtained from radial averages of the scattering pattern intensities.

UV/Vis spectra were recorded using an 8452A HP Diode Array Spectrophotometer. In kinetic studies performed, 0.2 ml of 6.8 nm nanoparticles (0.05 mg ml^{-1} in MeOH) were added dropwise to 1.8 ml of POSS solution (5mg ml^{-1} in MeOH). Scans were then taken at different time intervals. Similarly, solid films were prepared at the same concentrations by precipitating upon Mylar® films. Precipitation occurs over the 7 days, whereupon the excess solvent is decanted off and the films completely dried under argon. Scans were then taken by positioning the films at a 90° angle to the polarized beam to obtain the spectrum.

Acknowledgements

This research was supported by the National Science Foundation (CHE-0304173 and MRSEC facilities). Octa-ammonium POSS® was provided by Hybrid Plastics, Inc. B. L. F. thanks the ACS division of Organic Chemistry and Proctor and Gamble for the receipt of a 2003 graduate student fellowship.

References

1 Q. Zhou and T. M. Swager, *J. Am. Chem. Soc.*, 1995, **117**, 12 593; D. R. Walt, *Acc. Chem. Res.*, 1998, **31**, 267; R. A. Bissell, E. Cordova, A. E. Kaifer and J. F. Stoddart, *Nature*, 1994, **369**, 133.

2 J. Liu, J. Alvarez and A. E. Kaifer, *Adv. Mater.*, 2000, **12**, 1381; B. Kim, S. L. Tripp and A. Wei, *J. Am. Chem. Soc.*, 2001, **123**, 7955; B. L. Frankamp, O. Uzun, F. Ilhan, A. K. Boal and V. M. Rotello, *J. Am. Chem. Soc.*, 2002, **124**, 892.

3 POSS is a registered trademark of Hybrid Plastics, Inc.

4 J. D. Lichtenhan, in *Polymeric Materials Encyclopedia*, J. C. Salamone, ed., CRC Press, Boca Raton, FL, 1996, p. 7768; F. J. Feher, D. A. Newman and J. F. Walzer, *J. Am. Chem. Soc.*, 1989, **111**, 1741; J. F. Brown and L. H. Vogt, *J. Am. Chem. Soc.*, 1965, **87**, 4313.

5 J. J. Scwab and J. D. Lichtenhan, *Appl. Organomet. Chem.*, 1998, 707; R. A. Mantz, P. F. Jones, K. P. Chafee, J. D. Lichtenhan, J. W. Gilman, I. M. K. Ismail and M. J. Burmeister, *Chem. Mater.*, 1996, **8**, 1250.

6 L. Zheng, R. M. Kasi, R. J. Farris and E. B. Coughlin, *J. Polym. Sci., Part A: Polym. Chem.*, 2002, **40**, 885; L. Zheng, R. J. Farris and E. B. Coughlin, *Macromolecules*, 2001, **34**, 8034; H. Xu, S. W. Kuo, J. S. Lee and F. C. Chang, *Macromolecules*, 2002, **35**, 8788.

7 L. Zheng, A. J. Waddon, R. J. Farris and E. B. Coughlin, *Macromolecules*, 2002, **35**, 2375.

8 J. B. Carroll, A. J. Waddon, H. Nakade and V. M. Rotello, *Macromolecules*, 2003, **36**, 6289.

9 E. Jeoung, J. B. Carroll and V. M. Rotello, *Chem. Commun.*, 2002, 1510.

10 T. Cassagneau and F. Caruso, *J. Am. Chem. Soc.*, 2002, **124**, 8172.

11 J. B. Carroll, B. L. Frankamp and V. M. Rotello, *Chem. Commun*, 2002, 1892.

12 K. Naka, H. Itoh and Y. Chujo, *Nano Lett.*, 2002, **2**, 1183.

13 M. L. Sandrock and C. A. Foss, *J. Phys. Chem. B*, 1999, **103**, 11 398; B. Kim, S. L. Tripp and A. Wei, *J. Am. Chem. Soc.*, 2001, **123**, 7955.

14 W. F. Xie, *Eur. Phys. J. B*, 2000, **17**, 385; J. E. Martin, J. P. Wilcoxon, J. Odinek and P. Provencio, *J. Phys. Chem. B*, 2000, **104**, 9475.

15 X. M. Lin, C. M. Sorensen, K. J. Klabunde and G. C. Hadjipanayis, *Langmuir*, 1998, **14**, 7140; J. Jin, T. Iyoda, C. S. Cao, Y. L. Song, L. Jiang, T. J. Li and D. Ben Zhu, *Angew. Chem., Int. Ed.*, 2001, **40**, 2135.

16 T. H. Galow, U. Drechsler, J. A. Hanson and V. M. Rotello, *Chem. Commun.*, 2002, 1076.

17 U. Drechsler, N. O. Fischer, B. L. Frankamp and V. M. Rotello, *Adv. Mater.*, 2003, submitted.

18 q Values are converted into Å through the equation: $q = 2\pi/d$.

19 SPR is a physical process that can occur when plane-polarized light hits a metal film under total internal reflection conditions. See T. M. Davis and W. D. Wilson, *Anal. Biochem.*, 2000, **284**, 348.

20 J. J. Storhoff, A. A. Lazarides, R. C. Mucic, C. A. Mirkin, R. L. Letsinger and G. C. Schatz, *J. Am. Chem. Soc.*, 2000, **122**, 4640; A. A. Lazarides and G. C. Schatz, *J. Phys. Chem. B*, 2000, **104**, 460.

21 C. F. Bohren and D. R. Huffman, *Absorption and Scattering of Light by Small Particles*, Wiley, New York, 1983, p. 101.

22 W. Rechberger, A. Hohenau, A. Leitner, J. R. Krenn, B. Lamprecht and F. R. Aussenegg, *Optics Commun.*, 2003, **220**, 137.

23 T. Teranishi, S. Hasegawa, T. Shimizu and M. Miyake, *Adv. Mater.*, 2001, **13**, 1699.

24 M. Brust, M. Walker, D. Bethell, D. J. Schiffrin and R. Whyman, *J. Chem. Soc., Chem. Commun.*, 1994, 801.

25 R. S. Ingram, M. J. Hostetler and R. W. Murray, *J. Am. Chem. Soc.*, 1997, **119**, 9175.